Polymeric micelles as a new generation of anti-oxidant carriers*)

Rossella Arrigo[1)], Nadka Tzankova Dintcheva[1), **)], Giuliana Catalano[1)], Elisabetta Morici[1)], Giuseppe Cavallaro[2)], Giuseppe Lazzara[2)], Maurizio Bruno[3)]

DOI: dx.doi.org/10.14314/polimery.2017.525

Abstract: A promising strategy to immobilize a natural stabilizer in polymeric films is presented. Particularly, nevadensin (N, a natural basil flavonoid) molecules have been encapsulated in Pluronic F-127 micelles [F127, a triblock copolymer poly(ethylene oxide)-poly(propylene oxide)-poly(ethylene oxide)] and the obtained nanoparticles have been introduced in poly(ethylene glycol), PEG [otherwise known as poly(ethylene oxide), PEO]. In order to verify the effectiveness of the micelles as anti-oxidant carriers, PEG-based films have been subjected to artificial weathering. The encapsulation of anti-oxidant molecules allows the enhancement of N solubility in PEG, leading to advanced materials with enhanced photo-oxidative stability.

Keywords: polymeric micelles, anti-oxidant carriers, poly(ethylene oxide), photo-oxidative stability.

Micele polimerowe – nowa generacja nośników przeciwutleniaczy

Streszczenie: Przedstawiono obiecującą metodę immobilizacji naturalnych przeciwutleniaczy w materiale błon polimerowych. Cząsteczki naturalnego bazyliowego flawonoidu nevadensin (N) poddawano enkapsulacji w micelach tworzących się w roztworze triblokowego kopolimeru poli(tlenek etylenu)-poli(tlenek propylenu)-poli(tlenek etylenu), [PEO-PPO-PEO] – Pluronic F-127 (F127), a otrzymane nanocząstki wprowadzano do matrycy poli(tlenku etylenu) [PEO = PEG, poli(glikolu etylenowego)]. W celu zweryfikowania efektywności miceli jako nośników przeciwutleniaczy, błony wytworzone na bazie PEG poddano procesowi sztucznego starzenia. Stwierdzono, że enkapsulacja cząstek N w micelach F127 zwiększa rozpuszczalność nevadensinu w PEG, co umożliwia otrzymanie nowatorskiego materiału o zwiększonej stabilności fotooksydacyjnej.

Słowa kluczowe: micele polimerowe, nośniki przeciwutleniaczy, poli(tlenek etylenu), stabilność fotooksydacyjna.

In recent years, polymer nanotechnology based on block copolymers has emerged as an innovative technology in the field of drug delivery and gene therapy [1–3]. In particular, a promising example of a block copolymer extensively employed for such applications is represented by water-soluble, nonionic PEO-PPO-PEO [Pluronic, PEO: poly(ethylene oxide); PPO: poly(propylene oxide)] [4, 5]. Pluronic consists of hydrophobic and hydrophilic blocks that, above a critical temperature and concentration, self-aggregate in aqueous solutions to form spherical micelles with diameters ranging from 10 to 100 nm [6, 7]. The process of Pluronic micelle formation is affected by solution temperatures and pH [8], copolymer concentration [9] and molecular architecture [10]. Furthermore, the dimensions of the formed micelles, as well as the phase behavior of Pluronic solutions, can be properly varied through the introduction of different additives, such as sodium dodecyl sulfate [11]. Recently, the encapsulation of different drugs in Pluronic micelles has been broadly studied, since the core of the micelles provides a hydrophobic microenvironment suitable for solubilizing poorly water-soluble drugs [12–14]. All studies present in the literature agree that the presence of hydrophobic drug molecules affects the micellar dimensions and the gelation temperature [15]. For instance, the aggregation behavior of Pluronic micelles containing drugs of varying hydrophilicities has been investigated by Sharma *et al*., showing that the sizes of the micellar core and co-

[1)] University of Palermo, Department of Civil, Environmental, Aerospace, Materials Engineering, Viale delle Scienze, Ed. 6, 90128 Palermo, Italy.

[2)] University of Palermo, Department of Physics and Chemistry, Viale delle Scienze, Parco d'Orleans II, 90128 Palermo, Italy.

[3)] University of Palermo, Department of Biological, Chemical and Pharmaceutical Sciences and Technologies (STEBICEF), Viale delle Scienze, Parco d'Orleans II, 90128 Palermo, Italy.

*) This material was presented at 9th International Conference MoDeSt 2016, 4–8 September, 2016, Cracow, Poland.

**) Author for correspondence; e-mail: nadka.dintcheva@unipa.it

rona increase, while the aggregation number decreases, with higher drug hydrophobicities [16].

As is well known, the degradation phenomena of polymers and biopolymer-based materials can be efficiently prevented through the use of proper stabilizing systems during polymer processing [17–20]. Nevertheless, common stabilizers, above all naturally occurring stabilizing systems, show the tendency to migrate and volatilize under the typical temperatures used for polymer processing [21]. A promising strategy to overcome the issues related with stabilizer volatilization and/or degradation involves the immobilization and the encapsulation of the stabilizing systems [22]. Immobilization can be achieved through chemical linkage or physical absorption of stabilizer molecules onto solid nanoparticles; in this way, the nanoparticles, such as carbon nanotubes and clays, are used as anti-oxidant carriers within polymeric matrices [23], assuming a multi-functional action. The effectiveness of this innovative approach has been assessed by evaluating the immobilization of different stabilizing systems such as hindered phenols [24, 25], hindered amine light stabilizers [26] and naturally occurring stabilizing moieties [27, 28] in various nanoparticles. Polymer-based systems containing multi-hybrid nanoparticles showed enhanced thermo- and photo-oxidation resistance with respect to the systems containing free added stabilizers, due to the fact that immobilization allows the gathering of the anti-oxidant molecules at the interface between the host polymer matrix and nanoparticles, which represents the critical zone for the beginning of the polymer degradation [29].

Nevadensin (N) is a flavonoid isolated for the first time in 1966 from *Iva nevadensis* [30] and successively it has been shown to occur in several other plants belonging to the genera *Baccharis*, *Helianthus*, *Ocimum*, *Ononis*, *etc*. Nevadensin exhibits numerous biological activities such as anti-microbial, anti-inflammatory, anti-tubercular, hypotensive, anti-tumor and anti-cancer activities and its chemistry and bioactivity has been recently reviewed [31].

In this work, an innovative approach for the immobilization of a naturally occurring stabilizer is proposed. Specifically, Pluronic micelles have been prepared and used to encapsulate a suitable anti-oxidant for biopolymers, such as nevadensin. Moreover, the micelles without and with nevadensin have been introduced in PEG and the photo-oxidative stability of the formulated films has been accurately investigated.

EXPERIMENTAL PART

Materials

– Poly(ethylene glycol), PEG, with average molecular weight M_n = 20 000, melting point T_m = 63–66 °C was supplied by Sigma-Aldrich and used as received.

– Pluronic® F-127, F127, is a triblock copolymer PEO-PPO-PEO, where PEO is a poly(ethylene oxide); and PPO is a poly(propylene oxide), supplied by Sigma-Aldrich, having a critical micellar concentration, *CMC*, of 950–1000 ppm (~ 25 °C).

– Nevadensin (5,7-dihydroxy-6,8,4′-trimethoxyflavone), N, with the chemical formula reported in Scheme A.

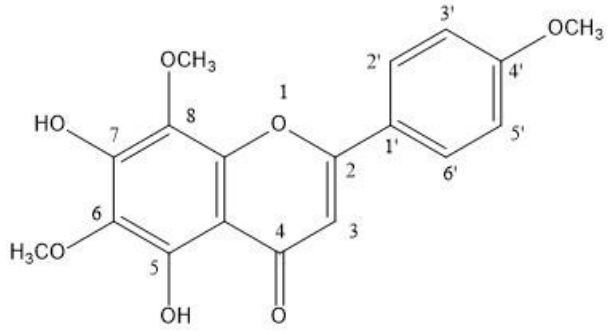

Scheme A

The isolation of nevadensin: 2.0 kg of powdered dry leaves of *Ocimum basilicum* L. were extracted with acetone (5 dm^3) for one week (three times). The solvent was completely removed under reduced pressure and 27 g of extract was obtained. The extract was subjected to dry-column chromatography over silica gel (300 g, deactivated with 15 % H_2O), 200 cm^3 fractions were collected as follows: 1–4 (petroleum ether), 5–8 (petroleum ether-EtOAc, 9 : 1), 9–12 (petroleum ether-EtOAc, 4 : 1), 13–16 (petroleum ether-EtOAc, 7 : 3), 17–20 (petroleum ether-EtOAc, 1 : l), 21–24 (petroleum ether-EtOAc, 2 : 3), 25–28 (petroleum ether-EtOAc, 1 : 4), 29–32 (EtOAc) and 33–36 (EtOAc-MeOH, 9 : 1). Fractions 13–16 were re-chromatographed over 40 g of silica gel (petroleum ether-EtOAc, 4 : 1) and then by preparative TLC (thin layer chromatography) ($CHCl_3$-Et_2O, 7 : 3) to give 2.25 g of nevadensin (N).

EIMS (electron ionization mass spectroscopy, 70 eV): *m/z* 344 $[M]^+$, 329 (base peak), 316 $[M–CO]^+$, 315 $[M–CO–H]^+$, 314 $[M–2Me]^+$, 312 $[M–2Me–2H]^+$, 301 $[M–CO–Me]^+$.

UV (ethanol): λ_{max} = 280, 335 nm; (+$AlCl_3$): 280, 310 (sh), 355 nm.

IR (KBr) ν = 3407, 3100, 2936, 2840, 1663, 1591, 1508, 1060, 1025 cm^{-1}.

^{1}H NMR ($CDCl_3$, 300 MHz; TMS): δ = 12.78 (1H, s, C5-OH), 7.89 (2H, dd, *J* = 2.7 Hz, 11.7 Hz, H-2′ and H-6′), 7.04 (2H, dd, *J* = 2.7 Hz, 11.7 Hz, H-3′ and H-5′), 6.58 (1H, s, C3-H), 4.04 (3H, s, C6-OCH_3), 4.02 (3H, s, C8-OCH_3), 3.90 (3H, s, C4′-OCH_3) ppm.

^{13}C NMR ($CDCl_3$, 75 MHz): δ = 164.2 (C-2), 104.2 (C-3), 183.4 (C-4), 148.8 (C-5), 131.5 (C-6), 149.2 (C-7), 128.5 (C-8), 146.2 (C-9), 105.0 (C-10), 124.0 (C-1′), 127.8 (C-2′, C-6′), 115.0 (C-3′, C-5′), 163.1 (C-4′), 61.4 (8-OCH_3), 62.3 (6-OCH_3), 56.0 (4′-OCH_3) ppm.

Pluronic nanoparticle preparation

An aqueous solution of Pluronic F-127 was prepared by adding the copolymer, in the form of a powder, to water and keeping the mixture under magnetic stirring for 24 hours at 25 °C. The copolymer concentration was fixed

at 5 wt %, which is significantly larger with respect to the critical micellar concentration (*CMC*) of F127 copolymer. Consequently, the copolymer dissolved in water generated the formation of the Pluronic nanoparticles with an hydrophobic pocket. Moreover, F127/PEG aqueous mixtures were prepared in order to study the influence of the PEG presence on the characteristics of Pluronic nanoparticles. To this purpose, the F127 concentration (5 wt %) was not altered while the amount of PEG was systematically changed within a wide interval. In detail, the F127 : PEG weight ratio ranged 0.00–1.67.

PEG-based film preparation

The films were prepared by using the casting method from water. Table 1 reports the weight compositions of the aqueous solutions used for the preparation of each investigated film, which were obtained after the evaporation of the solvent at 25 °C under vacuum. Then, the powder was pressed in a Carver laboratory press at room temperature under a pressure of 1500 psi (10.34 MPa) in order to form a film with a thickness of about 100 μm. It should be noted that the selected concentration of N is related to its specific solubility.

T a b l e 1. Weight compositions of the aqueous solutions used for the preparation of formulated films

Formulated film	Weight composition of the solution F127 : PEG : H_2O	Concentration of nevadensin mol/dm^3
F127	5 : 0 : 95	–
F127/N	5 : 0 : 95	$5.94 \cdot 10^{-5}$
PEG	0 : 12 : 88	–
PEG/N	0 : 12 : 88	$1.0 \cdot 10^{-5}$
PEG/F127	5 : 50 : 45	–
PEG/F127/N	5 : 50 : 45	$2.19 \cdot 10^{-4}$

Methods of testing

– Dynamic light scattering (DLS) experiments were carried out by means of a Zetasizer NANO-ZS (Malvern Instruments) at 25.0 ± 0.1 °C. The field-time autocorrelation functions were analyzed by ILT analysis, which provides the decay rate (Γ) profiles of the diffusive modes. For the translational motion, the collective diffusion coefficient is $D_t = \Gamma/q^2$ where q is the scattering vector given by $4\pi n\lambda^{-1}\sin(\theta/2)$ being n the solvent refractive index, λ the wavelength (632.8 nm) and θ the scattering angle (173°).

– The micro-DSC III 106 (SETARAM) (DSC, differential scanning calorimetry) under nitrogen flow in the range 5–80 °C with a scan rate of 0.6 °C/min was used to evidence the F127 self-assembling process in water. For all the aqueous solutions, a single endothermic phenomenon was observed and ascribed to the Pluronic micelle formation [32]. The critical micellar temperature (*CMT*) at the maximum of the peak, as well as the corresponding enthalpy from the integration of the thermogram, were determined. The baseline was subtracted according to the literature [33]. The measurements were carried out at a fixed F127 concentration by systematically changing the PEG amount.

– The steady-state pyrene fluorescence spectra added to the solid polymeric sample were recorded with a Horiba Spex-fluoroMax-3 spectrofluorometer. The excitation wavelength was set to 333 nm and the emission spectra recorded from 350 nm to 500 nm. Known aliquots of a solution of pyrene in acetone were carefully added into dark flasks by a Hamilton microsyringe. After acetone evaporation, the sample solutions were added and then the solvent was evaporated to obtain the solid polymer powder.

– ^{1}H and ^{13}C NMR spectra were recorded on a Bruker Avance series 300 MHz spectrometer, using the residual solvent signal (δ = 7.27 ppm in ^{1}H and δ = 77.00 ppm in ^{13}C for $CDCl_3$) as a reference. ^{13}C NMR assignments were determined by DEPT (distortionless enhancement by polarization transfer) spectra.

– Electron ionization mass spectroscopy EIMS was obtained with an Applied Biosystem API-2000 mass spectrometer.

– Merck silica gel (70–230 mesh, Merck No. 7734), deactivated with 15 % H_2O, was used for column chromatography (CC).

– Fourier transform infrared spectroscopy (FT-IR) was carried out on a Perkin Elmer FT-IR spectrometer (mod. Spectrum Two). The spectra were collected on films subjected to a continuous UV exposure. The photo-oxidation process has been carried out using a Q-UV weatherometer equipped with UVB lamps (313 nm) at a temperature of 40 °C.

– Scanning electron microscopy (SEM) was used to characterize the morphology of the polymeric films. SEM analysis of liquid nitrogen, radially fractured, gold sputtered surfaces were carried out on a Philips (Netherlands) ESEM XL30 microscope.

– Differential scanning calorimetry (DSC) was performed on PEG-based films, using a Perkin-Elmer DSC7 calorimeter. All experiments were run under dry N_2 with samples of about 10 mg in 0.04 cm^3 sealed aluminum pans. Four calorimetric scans (heating scan: 30–100 °C; cooling scan: 100–30 °C) were performed for each sample at a heating rate of 10 °C/min and a cooling rate of 20 °C/min.

– The degree of crystallinity (X_c) was calculated using:

$$X_c(\%) = \frac{\Delta H_m + \Delta H_{cc}}{\Delta H^\circ} \cdot 100 \qquad (1)$$

where: ΔH_m – the melting heat of the sample, ΔH_{cc} – the heat of cold crystallization, ΔH° – the heat of fusion for 100 % crystalline PEG (199.6 J/g) [34]. For samples containing Pluronic, the values of ΔH° have been corrected considering that the heat of fusion for 100 % crystalline Pluronic F-127 is 136.4 J/g [35].

RESULTS AND DISCUSSION

Characterization of nevadensin (N)

The EIMS spectrum of nevadensin shows a molecular ion at *m/z* 344 in agreement with the formula $C_{18}H_{16}O_7$. The infrared absorption bands indicate the presence of a bonded hydroxyl function (3407 cm^{-1}), chelated α,β-unsaturated carbonyl attached with aromatic nucleus (1663, 1591, 1508 cm^{-1}) and methoxy groups (1060 cm^{-1}). Its ^{1}H-NMR spectrum displays signals for an A_2B_2 aromatic system at 7.89 ppm (2H, dd, J = 2.7 Hz, 11.7 Hz, H-2′ and H-6′) and 7.04 ppm (2H, dd, J = 2.7 Hz, 11.7 Hz, H-3′ and H-5′), in agreement with a *para*-di-substituted benzene ring, for a bonded phenolic hydroxyl function at 12.78 ppm (1H, s), for a olefinic proton 6.58 ppm (1H, s, H-3) and for three methoxy groups at 4.04 ppm (3H, s, C6-OCH_3), 4.02 ppm (3H, s, C8-OCH_3) and 3.90 ppm (3H, s, C4′-OCH_3). All these data are in perfect agreement with those reported in literature [31].

Characterization of F127 micelles

The F127 is a copolymer able to self-assemble into micelles due to the difference in solubility temperature dependence of each block. As known in the literature, the presence of some additives can influence the self-assembling process of this PEO-PPO copolymer [36]. In order to verify the formation of F127 micelles in PEG matrix, the water + F127 and water + F127 + PEG mixtures have been prepared at different concentrations and temperatures and characterized through micro-calorimetry, dynamic light scattering and fluorescence. To investigate the F127 aggregation in micellar structures, the critical micellar temperature (*CMT*) was detected trough micro-calorimetry analysis at different PEG : F127 mass ratios, and the obtained results plotted in Fig. 1.

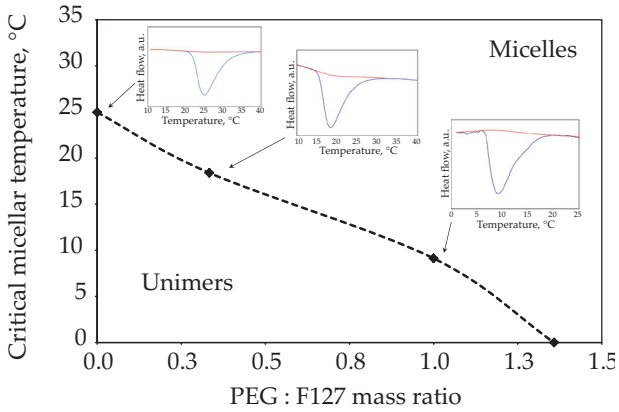

Fig. 1. Critical micellar temperature (*CMT*) *vs.* PEG : F127 mass ratio

Usually, the peak temperature is recognized as *CMT* while the peak area is related to the micellization enthalpy. It is interesting to highlight that the presence of PEG favors the formation of F127 micelles; particularly, as noticeable in the *CMT* trend *vs.* PEG : F127 mass ratio, for solutions with mass ratio PEG : F127 higher than 1.4, the aggregation in micelles occurs in the whole investigated temperature range. Furthermore, the beneficial effect of PEG presence on the F127 aggregation behavior is confirmed by DLS analysis, see Fig. 2.

For the F127 copolymer, it is possible to observe: (i) a single diffusive mode with an average hydrodynamic radius (R_h) of 4.6 nm at 15 °C, which is consistent with the unimeric F127 diffusion, see Fig. 2a; (ii) a double diffusive mode at 25 °C due to the diffusion of a small amount of unimeric F127 and a large amount of F127 micelles, see Fig. 2b. According to the literature [37], the radius of gyration (R_g) by a random coil model can be calculated as:

$$R_g = \sqrt{\frac{C_\infty \cdot N \cdot l^2}{6}} \qquad (2)$$

where: l – the monomer length (3.6 Å), C_∞ – the characteristic ratio in the limit of long chains (4.0 for PEO, PPO), N – the number of monomer [propylene oxide (PO) and ethylene oxide (EO)] units (PO + EO = 264 for F127). The value of the calculated radius of gyration for F127, considering the Eq. (2), is about 4.8 nm, which is very close to the experimental hydrodynamic radius of gyration (R_h) value. It is very important to note that the F127 micelles show a hydrodynamic radius of gyration R_h = 44 nm, as noticed by the second peak in the double diffusion mode at 25 °C. In contrast, PEG in water provides a faster diffu-

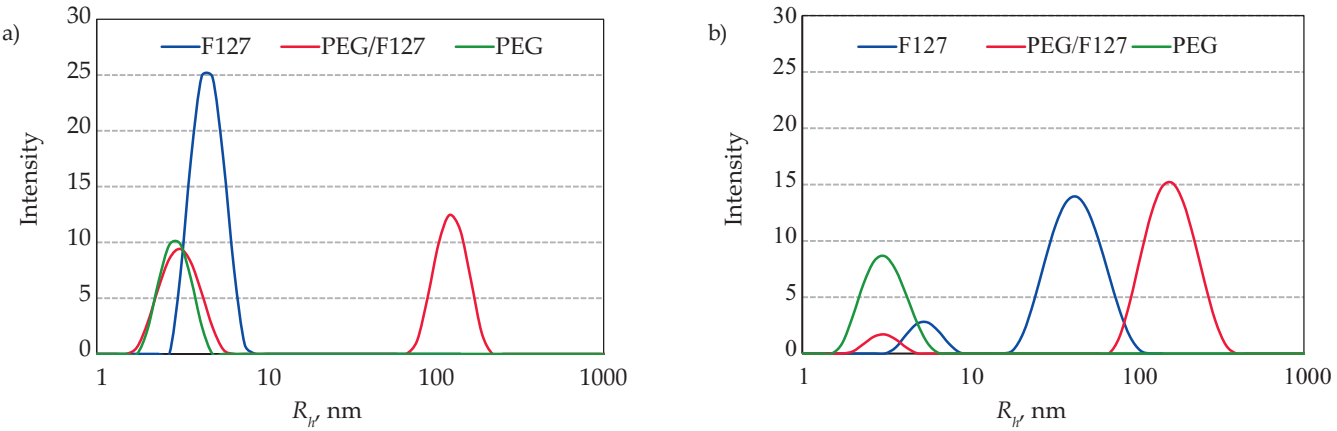

Fig. 2. Distribution of R_h for F127, PEG/F127 and PEG at: a) 15 °C, b) 25 °C

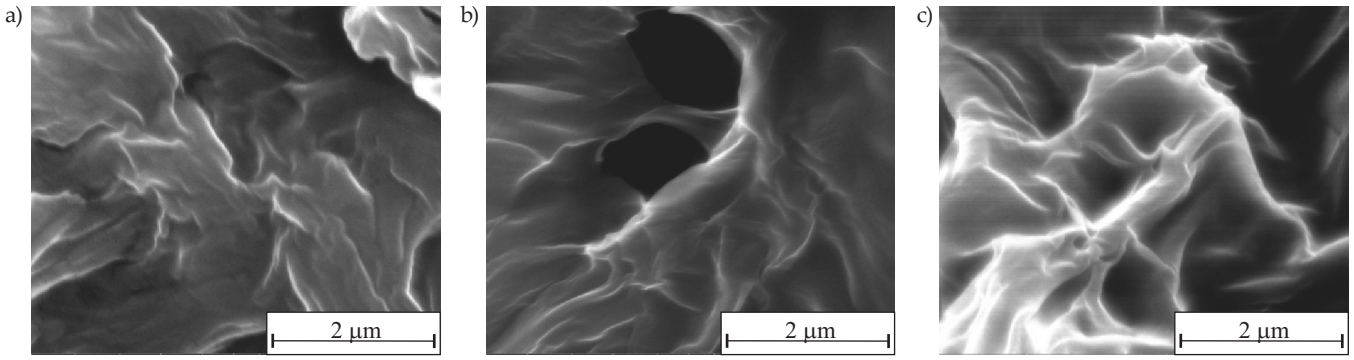

Fig. 3. SEM observations of: a) neat PEG, b) PEG/F127, c) PEG/F127/N

T a b l e 2. Cold crystallization (T_{cc}) and melting (T_m) temperatures, relative enthalpies (ΔH_{cc}, ΔH_m) and crystallinity degree (X_c) of PEG-based films

Sample	T_{cc}, °C	ΔH_{cc}, J/g	T_m, °C	ΔH_m, J/g	X_c, %
PEG	35.9	-131.8	60.4	147.2	7.7
PEG/N	36.5	-83.7	56.7	96.0	6.1
PEG/F127	39.8	-47.2	58.5	55.0	3.9
PEG/F127/N	36.5	-21.5	55.6	26.5	2.5

sion with R_h = 3.1 nm at both investigated temperatures. Furthermore, it is worth noting that PEG presence in PEG/F127 samples cause, on one hand, the favoring of the F127 aggregation also at low temperature, *i.e.*, at 15 °C, see the double diffusive mode in Fig. 2a. On the other hand, the R_h of F127 micelles shifts from *ca.* 120 nm at 15 °C to *ca.* 160 nm at 25 °C, highlighting again the beneficial effect of PEG in the F127 micelle formation.

To verify the maintenance of the F127 micellar structure in the solid state, water + F127 + PEG mixture, in presence of pyrene, was dried and the obtained solid film was investigated through fluorescence spectroscopy, using pyrene as a fluorescence probe. Indeed, it is well known that, analyzing the emission spectrum of pyrene, the ratio between the intensity (I) of the first and the third vibrational band depends significantly on the medium polarity. For example, the ratio I_1/I_3 is 1.8 in water and 1.2–0.8 in hydrophobic environments. The obtained spectrum shows five specific bands, with the first and the third centered at 373 nm and 384 nm, respectively. For the PEG/F127 system, the calculated ratio I_1/I_3 is 0.90, very close to that of pure F127 (I_1/I_3 = 0.95), confirming the existence of hydrophobic domains for dried F127 in presence of PEG.

Characterization and photo-oxidation resistance of PEG-based films

To evaluate the morphology of PEG-based films, SEM observations were carried out on nitrogen fractured surfaces. SEM micrographs reported in Fig. 3 show that the addition of empty and nevadensin-containing micelles almost does not affect the PEG morphology. It is worth noting that, due to the similarity between PEG and F127, the micellar structures cannot be observed as a separate phase.

The effect of the presence of F127 micelles on the thermal behavior of PEG was investigated through differential scanning calorimetry. In Table 2, the data collected during the second heating scan are reported.

As known in the literature, neat PEG experiences cold crystallization phenomena due to a crystallization process occurring above the glass transition temperature.

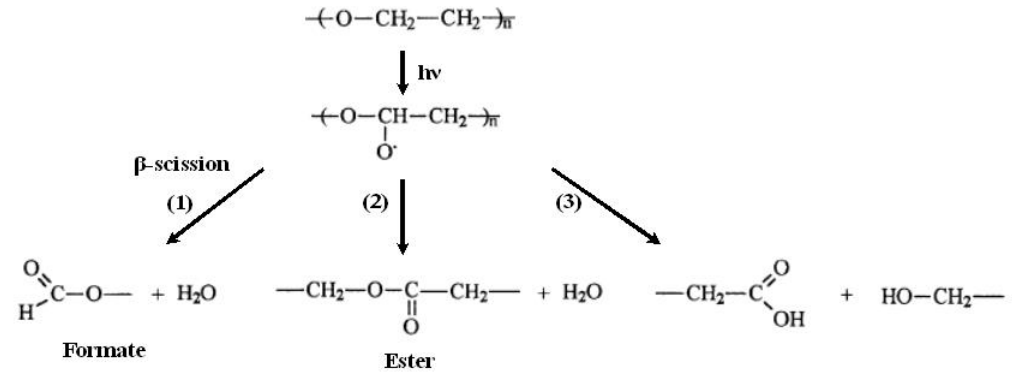

Scheme B

The crystallinity degree of PEG [calculated using Eq. (1)] decreases due to the presence of N, and even more in the presence of empty and nevadensin-containing F127 micelles, probably because of the reduced mobility of PEG macromolecules.

To investigate the photo-oxidation resistance of PEG-based films, the samples were subjected to accelerated aging and the progress of the degradation was monitored through FT-IR spectroscopic analysis. In agreement with the literature, PEG degrades upon UV exposure to form radical species that, in turn, are able to react with macromolecules [38]. The formed radicals, as shown in the degradation pathway of neat PEG reported in Scheme B, produce peroxy radicals by reaction with oxygen, and hydroperoxides by abstraction of hydrogen atoms.

During the hydroperoxide decomposition, which occurs following three degradation routes, formates, esters, alcohols and carboxylic acids are formed. Due to the formation of these oxygen containing species, a new band in the range 1850–1600 cm^{-1} in the FT-IR spectrum appears, see inset in Fig. 4, whose intensity increases as a function of the exposure time.

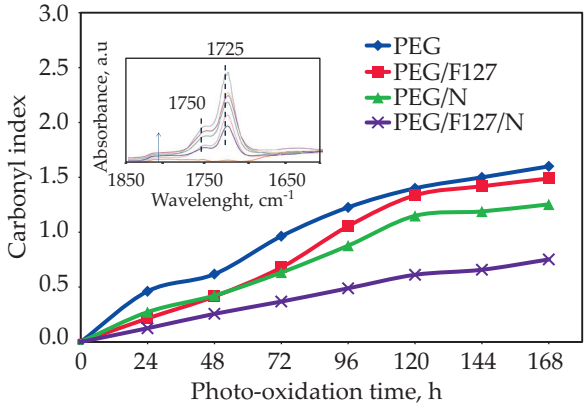

Fig. 4. Carbonyl index (*CI*) as a function of exposure time of PEG-based films; the inset reports the FT-IR spectra in the carbonyl region of neat PEG at different exposure times

To monitor the progress of the degradation phenomena, the carbonyl index (*CI*), calculated as the ratio between the area of the carbonyl band (1850–1600 cm^{-1}) and the area of the reference peak (1965 cm^{-1}, taking into account the sample thickness variation), was considered. The trend of *CI* for neat PEG and PEG-based films is plotted in Fig. 4 as a function of the photo-oxidation time. Clearly, the photo-oxidation behavior of PEG is not influenced by the presence of F127 micelles. Concerning the system containing free N molecules, the last are able to exert a protective action against the photo-oxidation of PEG-based films due to N's inherent anti-oxidant activity. The encapsulation of N in F127 micelles leads to the formulation of PEG-based film with enhanced photo-oxidation resistance. The latter can be understood considering the improved solubility of N molecules in PEG-based on data reported in the experimental part, see Table 1. Overall, the obtained results confirm the effectiveness of the proposed strategy for the formulation of PEG-based films with prolonged durability.

CONCLUSIONS

Nevadensin molecules have been successfully encapsulated in F127 micelles and dispersed in PEG-based film, with the aim to obtain photo-oxidative resistant films. To assess the effectiveness of the proposed approach for stabilization, thin PEG-based films have been subjected to prolonged UV exposure. The obtained results suggest that the encapsulation of N molecules in F127 micelles enhances their solubility in a polymeric matrix. The PEG/F127/N film shows improved photo-oxidation resistance with respect to the unstabilized PEG-based films and to the system containing free N molecules. Therefore, the proposed use of polymeric micelles as anti-oxidant carrier can be considered a viable route for the formulation of polymeric film with improved photo-oxidation stabilities.

REFERENCES

[1] Batrakova E.V., Kabanov A.V.: *Journal of Controlled Release* **2008**, *130*, 98. http://dx.doi.org/10.1016/j.jconrel.2008.04.013
[2] Fattahpour S., Shamanian M., Tavakoli N. *et al.*: *Journal of Applied Polymer Science* **2015**, *132*, 42 241. http://dx.doi.org/10.1002/app.42241
[3] Kabanov A.V., Lemieux P., Vinogradow S., Alakhov V.: *Advanced Drug Delivery Reviews* **2002**, *54*, 223. http://dx.doi.org/10.1016/S0169-409X(02)00018-2
[4] Basak R., Bandyopadhyay R.: *Langmuir* **2013**, *29*, 4350. http://dx.doi.org/10.1021/la304836e
[5] Sahu A., Kasoju N., Goswami P., Bora U.: *Journal of Biomaterials Applications* **2011**, *25*, 619. http://dx.doi.org/10.1177/0885328209357110
[6] Singh V., Khullar P., Dave P.N., Kaur N.: *International Journal of Industrial Chemistry* **2013**, *4*, 12. http://dx.doi.org/10.1186/2228-5547-4-12
[7] Kabanov A.V., Nazarova I.R., Astafieva I.V. *et al.*: *Macromolecules* **1995**, *28*, 2303. http://dx.doi.org/10.1021/ma00111a026
[8] Wanka G., Hoffmann H., Ulbricht W.: *Macromolecules* **1994**, *27*, 4145. http://dx.doi.org/10.1021/ma00093a016
[9] Alexandridis P., Nivaggioli T., Hatton T.A.: *Langmuir* **1995**, *11*, 1468. http://dx.doi.org/10.1021/la00005a011
[10] Mortensen K., Pedersen J.S.: *Macromolecules* **1993**, *26*, 805. http://dx.doi.org/10.1021/ma00056a035
[11] Jansson J., Schillén K., Olofsson G. *et al.*: *The Journal of Physical Chemistry B* **2004**, *108*, 82. http://dx.doi.org/10.1021/jp030792u
[12] Sharma P.K., Bhatia S.R.: *International Journal of Pharmaceutics* **2004**, *278*, 361. http://dx.doi.org/10.1016/j.ijpharm.2004.03.029

[13] Lavasanifar A., Samuel J., Kwon G.S.: *Advanced Drug Delivery Reviews* **2002**, *54*, 169. http://dx.doi.org/10.1016/S0169-409X(02)00015-7
[14] Foster B., Cosgrove T., Hammounda B.: *Langmuir* **2009**, *25*, 6760. http://dx.doi.org/10.1021/la900298m
[15] Guo L., Colby R.H., Thiyagarajan P.: *Physica B: Condensed Matter* **2006**, *385*, 685. http://dx.doi.org/10.1016/j.physb.2006.05.291
[16] Sharma P.K., Reilly M.J., Jones D.N.: *Colloids and Surfaces B: Biointerfaces* **2008**, *61*, 53. http://dx.doi.org/10.1016/j.colsurfb.2007.07.002
[17] Zaborski M., Masek A., Chrzescijanska E.: *Polimery* **2011**, *56*, 558.
[18] Dintcheva N.Tz., La Mantia F.P., Arrigo R.: *Journal of Polymer Engineering* **2014**, *34*, 441. http://dx.doi.org/10.1515/polyeng-2013-0169
[19] Lipiński W., Ogonowski J., Uhniat M.: *Polimery* **2002**, *10*, 713.
[20] Tátraaljai D., Földes E., Pukánszky B.: *Polymer Degradation and Stability* **2014**, *102*, 41. http://dx.doi.org/10.1016/j.polymdegradstab.2014.02.010
[21] Lundbäck M., Strandberg C., Albertsson A. *et al*.: *Polymer Degradation and Stability* **2006**, *91*, 1071. http://dx.doi.org/10.1016/j.polymdegradstab.2005.07.010
[22] Dintcheva N.Tz., Catalano G., Arrigo R. *et al*.: *Polymer Degradation and Stability* **2016**, *134*, 194. http://dx.doi.org/10.1016/j.polymdegradstab.2016.10.008
[23] Arrigo R., Dintcheva N.Tz., Guenzi M., Gambarotti C.: *Materials Letters* **2016**, *180*, 7. http://dx.doi.org/10.1016/j.matlet.2016.05.096
[24] Dintcheva N.Tz., Arrigo R., Gambarotti C. *et al*.: *Journal of Applied Polymer Science* **2015**, *132*, 42 420. http://dx.doi.org/10.1002/app.42420
[25] Dintcheva N.Tz., Al-Malaika S., Morici E.: *Polymer Degradation and Stability* **2015**, *122*, 88. http://dx.doi.org/10.1016/j.polymdegradstab.2015.09.005
[26] Dintcheva N.Tz., Arrigo R., Morici E. *et al*.: *Composites Part B: Engineering* **2015**, *82*, 196. http://dx.doi.org/10.1016/j.compositesb.2015.07.017
[27] Dintcheva N.Tz., Arrigo R., Gambarotti C. *et al*.: *Carbon* **2014**, *74*, 14. http://dx.doi.org/10.1016/j.carbon.2014.02.074
[28] Arrigo R., Dintcheva N.Tz., Guenzi M. *et al*.: *Polymer Degradation and Stability* **2015**, *115*, 129. http://dx.doi.org/10.1016/j.polymdegradstab.2015.02.014
[29] Dintcheva N.Tz., Arrigo R., Carroccio S. *et al*.: *European Polymer Journal* **2016**, *75*, 525. http://dx.doi.org/10.1016/j.eurpolymj.2016.01.002
[30] Farkas L., Nogradi M., Sudarsanam V., Herz W.: *The Journal of Organic Chemistry* **1966**, *31*, 3228. http://dx.doi.org/10.1021/jo01348a031
[31] Brahmachari G.: *International Journal of Green Pharmacy* **2010**, *4*, 213. http://dx.doi.org/10.4103/0973-8258.74128
[32] Chiappisi L., Lazzara G., Gradzielski M., Milioto S.: *Langmuir* **2012**, *28*, 17 609. http://dx.doi.org/10.1021/la303599d
[33] Malakhov D.V., Abou Khatwa M.K.: *Journal of Thermal Analysis and Calorimetry* **2007**, *87*, 595. http://dx.doi.org/10.1007/s10973-006-7702-3
[34] Cavallaro G., De Lisi R., Lazzara G., Milioto S.: *Journal of Thermal Analysis and Calorimetry* **2013**, *112*, 383. http://dx.doi.org/10.1007/s10973-012-2766-8
[35] Gerasimov A.V., Ziganshin M.A., Gorbatchuk V.V.: *World Applied Sciences Journal* **2013**, *24*, 920. http://dx.doi.org/10.5829/idosi.wasj.2013.24.07.13235
[36] Lazzara G., Milioto S., Gradzielski M.: *Physical Chemistry Chemical Physics* **2006,** *8*, 2299. http://dx.doi.org/10.1039/B516242B
[37] Flory P.J.: "Statistical Mechanics of Chain Molecules", Interscience Publishers, New York 1969.
[38] Morlat S., Gardette J.L.: *Polymer* **2001**, *42*, 6071. http://dx.doi.org/10.1016/S0032-3861(01)00084-2

Received 8 XII 2016.